

Figure S1. PKA and p38 MAPK activities in adipocytes derived from primary MEFs (WT and LXRα^{-/-}). Differentiated MEFs were treated with 10 μM Iso for 5 min for PKA activity (**A**) and 10 min for p38 MAPK activity (**B**) as described in Experimental Procedures. Kinase activities were measured in whole-cell lysates using Kemptide (for PKA activity) and GST-ATF2 (for p38 MAPK activity) as substrates. The fluorescent bands were visualized with Typhoon 9410 variable mode Imager from GE Healthcare (Piscataway, NJ), and quantified by densitometry analysis using ImageQuant 5.2 software from Molecular Dynamics (Piscataway, NJ). Results are presented as means ± SEM for 3 independent experiments for each measure. *p<0.05 vs baseline control of WT; †p<0.05, ††p<0.001 vs baseline control of LXRα^{-/-} (1-way ANOVA).

Table S1. Nucleotide sequences of the primers used in real-time PCR.

Gene	Primer Sequence (5' - 3')
GABP α / NRF-2A	TCTATGGCCTGGCTTACACA (For) AAATTGAGATCGACGGGACT (Rev)
GABP β 1 / NRF-2B1	CAATACTTGCTGTCCATCGG (For) TGCACTCCATACCAACCAGT (Rev)
GABP β 2 / NRF-2B2	TTGTCTCCTCTGCAACCTGA (For) TTGGCCAGCCATTTATTGTA (Rev)
Cytochrome C (Cytc)	TCTTATGCTTGCCTCCCTTT (For) AGCCCGGAACGAATTAAA (Rev)
COX2	AGCATTGGCCATAGAATAACC (For) CATCCCAGGCCGACTAAAT (Rev)
COX4	CTGGATGCGGTACAACCTGAA (For) CGCTGAAGGAGAAGGAGAAG (Rev)
PGC-1 α	TGCTCTTTGCGGTATTCATC (For) TCACGTTCAAGGTCACCCTA (Rev)
PGC-1 β	TTCCTCAACTATCTCTCTGACACG (For) TCTGGCAAGTCAGCACACA (Rev)
Ucp1	AGAAGCCACAAACCCTTTGA (For) AGTACCCAAGCGTACCAAGC (Rev)
RIP140	CTCAGCTTCCTTTCCACAT (For) CAAACGCACGTCACTATCGT (Rev)
GAPDH	TGCACCACCAACTGCTTAG (For) GATGCAGGGATGATGTTTC (Rev)

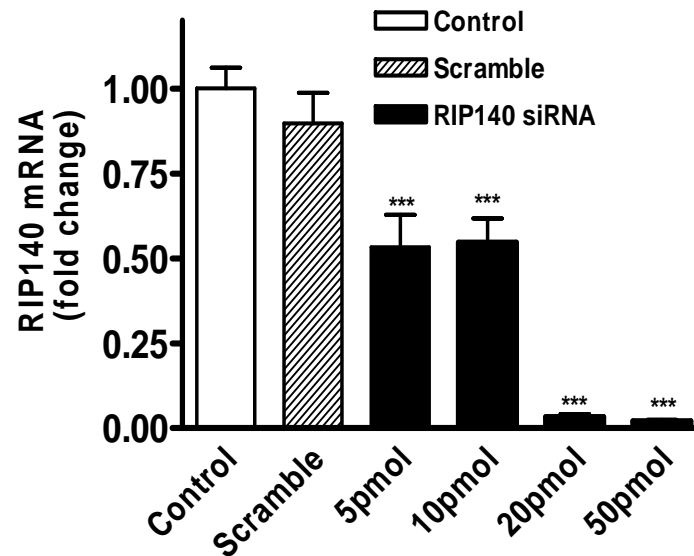


Figure S2. Gene silencing in HIB-1B cells. Increasing amounts of RIP140 short interfering RNA (siRNA) were transfected into HIB-1B cells as described in Experimental Procedures. The figure shows the fractional change in RIP140 as measured by RT-PCR with Taqman probes compared with mock transfection and scramble siRNA as negative control. *** $p < 0.001$ vs control (1-way ANOVA; $n = 6$).

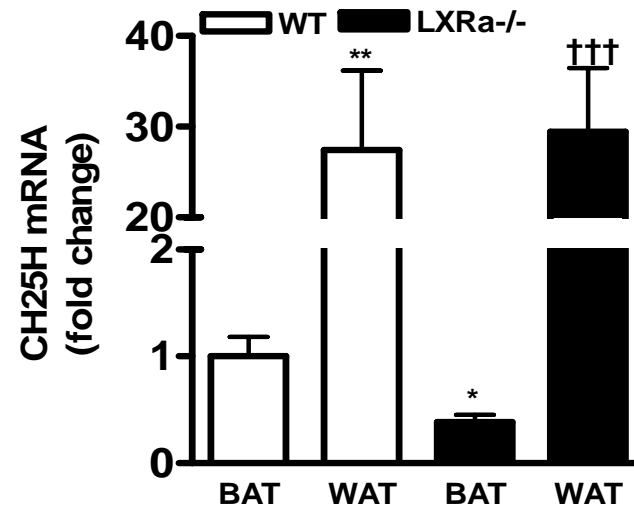


Figure S3. Cholesterol 25-hydroxylase (CH25H) is more abundant in WAT than BAT. Taqman real-time PCR analysis of CH25H gene expression in BAT and WAT of WT and LXRα-/- mice. All statistical comparisons of expression levels are relative to WT BAT. n=6, *p<0.05, **p<0.01 vs BAT in WT; †††p<0.001 vs BAT in LXRα-/- (1-way ANOVA).

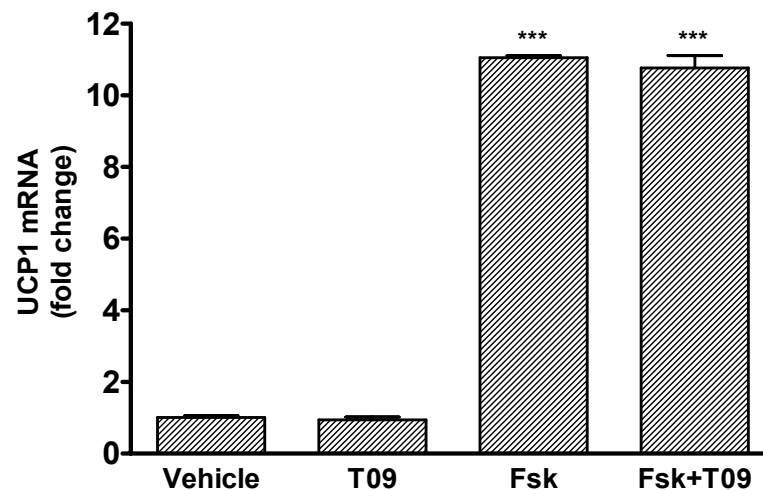
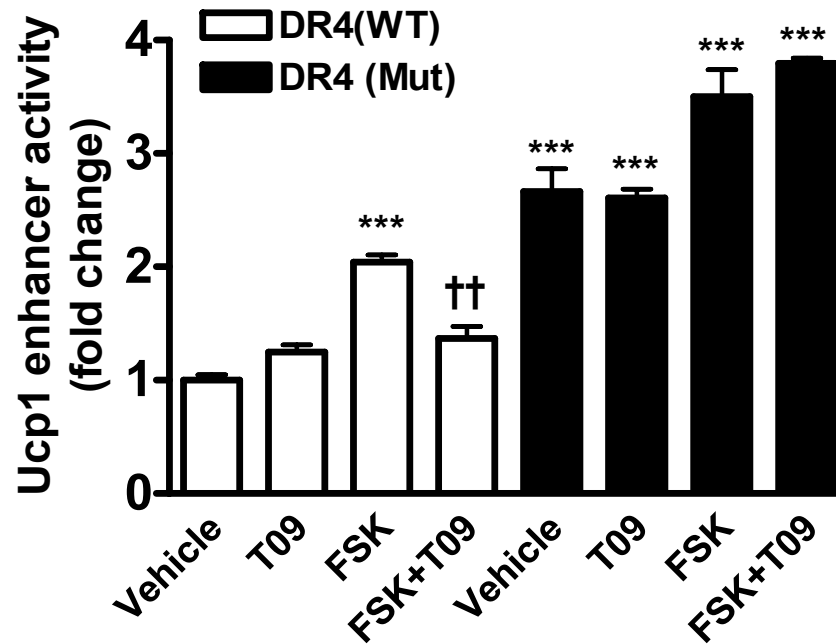


Figure S4 Suppression of cAMP-stimulated Ucp1 expression is absent in $LXR\alpha^{-/-};\beta^{-/-}$ adipocytes. Differentiated MEFs were treated for 6 hr with vehicle (DMSO), 5 μ M T09, 10 μ M FSK and FSK plus T09 as indicated. RT-PCR analysis of Ucp1 gene expression. Results are mean \pm SEM relative to vehicle-treated cells for each genotype. *** $p < 0.001$ vs vehicle-treated control (1-way ANOVA; $n = 4-6$).



FigureS5. Activated LXR α suppresses cAMP-stimulated Ucp1 enhancer activity through a DR-4 element. Transient transfection of HIB-1B cells with tk-CAT reporter genes containing the 220-bp enhancer element from the mouse Ucp1 gene with wild type (DR4 WT) or mutant DR-4 sequences (DR-4 Mut, as described in Fig 6B). Results presented are mean \pm SEM. **p<0.01, ***p<0.001 vs basal untreated WT-DR-4; ††p<0.01, vs FSK-treated WT-DR-4 (1-way ANOVA; n = 3).